Published in final edited form as:
J Proteome Res. 2008 August ; 7(8): 3127–3136. doi:10.1021/pr800264t.

A Proteomics Grade Electron Transfer Dissociation-enabled Hybrid Linear Ion Trap-orbitrap Mass Spectrometer

Graeme C. McAlister[1], **W. Travis Berggren**[5], **Stevan Horning**[4], **Alexander Makarov**[4], **Doug Phanstiel**[1], **Jens Griep-Raming**[4], **George Stafford**[3], **Danielle L. Swaney**[1], **John E. P. Syka**[3], **Vlad Zabrouskov**[3], and **Joshua J. Coon**[1,2]

1 *Department of Chemistry, University of Wisconsin, Madison, WI 53706*

2 *Department of Biomolecular Chemistry, University of Wisconsin, Madison, WI 53706*

3 *Thermo Scientific San Jose, CA*

4 *Thermo Scientific, Bremen, Germany*

5 *WiCell Research Institute, Madison, WI 53706*

Abstract

Here we describe the modification of a quadrupole linear ion trap-orbitrap hybrid (QLT-orbitrap) mass spectrometer to accommodate a negative chemical ionization (NCI) source. The NCI source is used to produce fluoranthene radical anions for imparting electron transfer dissociation (ETD). The anion beam is stable, robust, and intense so that a sufficient amount of reagents can be injected into the QLT in only 4 - 8 ms. Following ion/ion reaction in the QLT, ETD product ions are mass-to-charge (*m/z*) analyzed in either the QLT (for speed and sensitivity) or the orbitrap (for mass resolution and accuracy). Here we describe the physical layout of this device, parametric optimization of anion transport, an evaluation of relevant ETD figures of merit, and the application of this instrument to protein sequence analysis. Described proteomic applications include complex peptide mixture analysis, post-translational modification (PTM) site identification, isotope-encoded quantitation, large peptide characterization, and intact protein analysis. From these experiments we conclude the ETD-enabled orbitrap will provide the proteomic field with several new opportunities and represents an advance in protein sequence analysis technologies.

Introduction

Hybrid mass spectrometers that combine sensitive, fast scanning quadrupole linear ion traps with high resolving power Fourier transform mass analyzers (e.g., QLT-orbitrap and ion cyclotron resonance, QLT-FT-ICR) have become a central tool for many MS-based proteomic efforts.[1–5] The combination of speed, sensitivity, high mass accuracy and resolving power results in elevated peptide identification confidence – especially for post-translational modification (PTM) analysis – and is advantageous for large peptide and whole protein analysis (e.g., top-down). Tandem mass spectrometry is a critical component of all the above systems and is implemented almost exclusively via some form of collisional-activation (CAD).[6, 7] In addition to CAD, standalone ion traps afford the opportunity to perform electron transfer dissociation (ETD) – a technique that generally preserves labile posttranslational (PTMs) and is indifferent less sensitive to amino acid composition or order, and peptide length.[8–17] Performing ETD on a chromatographic time-scale, however, relies on a stable, intense source

Correspondence to: Joshua J. Coon.

of high purity anionic reagents. Such an anion source – negative chemical ionization (NCI) [18, 19] – can be easily fitted to the rear (unoccupied) end of a standalone linear quadrupole ion trap, but FT analyzers and associated ion transmission optics occupy this position on orbitrap and QLT-FT-ICR hybrids.

Recently we reported on the modification of a linear ion trap-orbitrap hybrid mass spectrometer (QLT-orbitrap) to perform electron transfer dissociation (ETD).[20] That work, based on the approach of Liang et al. adapting ETD to a hybrid quadrupole time-of-flight mass spectrometer, used a pulsed, dual electrospray ion source to generate both cationic peptide precursors and anionic reagent species (front-end, FE-ETD).[21, 22] Switching between cation and reagent anion injection schemes consumed a few hundred milliseconds – one of two major drawbacks of that implementation. Later we lowered switching time duration by use of a dual electrospray setup with rapid physical switching (~ 30 ms) of the separate nanoESI emitters.[23] Still both approaches suffered from poor anion electron transfer efficiency. That is, the anionic reagent generated via negative ESI had a relatively low propensity to engage in electron transfer ion/ion reactions, preferring instead to react via a proton transfer chemistry with a partition ratio of (~ 1:7). Taken together these shortcomings resulted in the acquisition of ETD tandem mass spectra with low signal-to-noise (S/N) ratios and long acquisition times (~ 6 seconds).

To eliminate these shortcomings we adapted a QLT-orbitrap mass spectrometer to accommodate a NCI source. The source provides a generous flux of fluoranthene radical anions for rapid, high efficiency electron transfer reactions. In this arrangement an octopole serves as a bridge to transport the radical anions from the NCI source to the rear side of the hybrid mass spectrometer's c-trap. From there the existing ion optics, an octopole and the c-trap, serve to transmit the anions to their final destination – the linear ion trap. Here we describe the physical layout of this device, parametric optimization of anion transport, an evaluation of relevant ETD figures of merit, and the application of this instrument to protein sequence analysis.

Materials and Methods

Instrumentation

All experiments were performed using a commercially available hybrid LTQ–Orbitrap mass spectrometer (Thermo Scientific, Bremen, Germany) that was modified to conduct ETD reactions (Fig. 1). This instrument consists of three independent ion trapping devices – two radio frequency ion traps (QLT and c-trap) and the electrostatic orbitrap. During typical operation, ion manipulation events are conducted in the QLT (e.g., precursor isolation, ion/ion reaction, etc.). The analyte ion population is then either mass-to-charge (*m/z*) analyzed in the QLT or sent to the orbitrap, via the c-Trap, for high resolution and mass accuracy analysis.

Instrument modifications to support ETD consisted of two main alterations: (1) the coupling of a NCI source to the c-trap using an octopole and (2) modification of the QLT to enable ion/ion chemical reactions. ETD reagent anions, formed in the NCI source, commute to the QLT via the added octopole, the c-trap, and another transfer octopole. Device voltages and pressures were optimized to allow for efficient anion injection, *vide infra*. ETD fragmentation was enabled by modification of the QLT to allow application of a supplementary RF voltage on the trap end lenses.[14] This alteration allows ions of opposite polarity to be trapped in the same space at the same time (charge-sign independent trapping – CSIT), transforming the QLT into an ion/ion reaction vessel. In addition to these hardware modifications, the firmware and software of the instrument was modified to support the new components and scan types.

During a typical ETD MS/MS scan, analyte cations are injected into the QLT for subsequent precursor cation isolation (Fig. 1 – Voltages 1). Next, ETD reagent anions are injected into the QLT (Fig. 1 – Voltages 2) where they are subsequently reacted with the isolated precursor

using CSIT (Fig. 1 – Voltages 3). Product ions generated by these reactions are then *m/z* analyzed in either the QLT or the orbitrap. Instrument modifications are supported in such a manner that scan details, such as anion AGC target values, ETD reaction times and orbitrap transient acquisition times (*m/z* resolution), are easily varied through the user interface.

Sample Preparation, Chromatography, and Data Acquisition

All experiments were performed using self-prepared microcapillary columns – reversed-phase C_{18} material (Alltima 5 μm beads from Alltech Associates, Inc., Deerfield IL) with integrated nano-electrospray emitters (nESI) as previously described.[24] Chromatographic separations were performed using an Agilent 1100 series HPLC and a micro-T for flow splitting (Agilent Technologies, Palo Alto CA). Solvent A consisted of 100 mM of aqueous acetic acid; solvent B consisted of 70:30 acetonitrile to water with 100 mM of acetic acid. Unless otherwise noted, all chemicals were from Sigma (St. Louis, MO).

Histone H4—Human embryonic stem cells (human ES cells, H1 line) were grown and histone H4 was purified as previously described.[25] Purified histone H4 samples were digested overnight with Asp-N at a substrate-to-enzyme ratio of 20:1 at pH 8 and a temperature of 37 degrees before MS analysis (Roche, Nutley, NJ). Approximately 10 pmol of histone H4 digest was bomb loaded onto a microcapillary pre-column and eluted from a nanoscale ESI column by a 0–25% gradient in 40 minutes. ETD MS/MS experiments were performed on precursors of interest with mass detection in both the ion trap and orbitrap mass analyzers (separately). The mass spectrometer, for this and the following applications, was operated with the following settings: isolation width = 2.0, reaction time = 50 ms, reagent ion AGC target = 100,000, ion trap MSN AGC target = 80,000, orbitrap MSN AGC target = 300,000, microscans = 1.

SILAC labeled phosphospeptide—Human ES cells (H9 line) were grown as described above and expanded to 2×10^8 cells. Half of these cells were grown on feeder independent media (TeSR), as previously described, in which all arginine residues contained 6 C^{13} atoms (stable isotope labeling with amino acids in cell culture, SILAC, Fisher Scientific, Pittsburgh, PA).[26] Proteins from two cellular populations were mixed at a 1:1 ratio, followed by digestion with trypsin (Promega, Madison, WI) at 37°C for 1 hour. The sample was then desalted in a C_{18} SepPak cartridge (Waters, Milford, MA) and enriched for phosphopeptides using immobilized metal affinity chromatography (IMAC). These peptides were then eluted from a micro-capillary column by a 0–50 % B gradient in 180 min. MS analysis was performed in the orbitrap followed by selection of the eight most abundant ions for ETD interrogation and subsequent *m/z* analysis in the ion trap.

Other human cells—Human glioblastoma cells (U87MG line) were lysed by sonication and centrifuged. An 3.6 mg aliquot of the protein containing supernatant was reduced, alkylated, and digested with endoproteinases lysineC overnight (Princeton separations, Adelphia, NJ). The sample was then acidified and desalted on a 500 mg tC_{18} SepPak cartridge (Waters, Milford, MA). Strong cation exchange fractionation of the sample was carried out as previously described.[27] Following desalting on a 100mg tC_{18} SepPak cartridge (Waters, Milford, MA) a fration was chromatographically separated using a Waters NanoAcquity HPLC in which solvent A was 0.2% formic acid (Thermo Fisher Scientific, Waltham, MA) and solvent B was 70% acetonitrile in 0.2% formic acid. These peptides were eluted from a micro-capillary column by a gradient from 0–20% B in 10 minutes, and then to 70% B in 110 minutes. All MS scans were performed in the orbitrap followed by ETD interrogation of the four most abundant precursors. Each precursor was interrogated twice by ETD twice – once using the ion trap and once with the orbitrap (30,000 nominal resolving power) for product ion *m/z* analysis.

Database Searching—Spectra generated from the *Saccharomyces cerevisiae* experiments were searched against the yeast subset of the NCBI database using the Open Mass Spectrometry Search Algorithm (OMSSA).[28] For all searches parameters were set to consider a static modification of + 57 Da on cysteine residues (carbamidomethylation) and a differential modification of +16 Da on methionine residues. False positive rate was determined using the forward-reverse database method described by Gygi et al.[29]

Results and Discussion

Instrument design and characterization

The driving criterion of this work was to implement a stable, intense source of reagent anions having high electron transfer efficiencies on a QLT-orbitrap mass spectrometer. To do this we elected to employ an NCI source, analogous to the original and commercial implementation of ETD on a stand alone QLT instruments. Figure 1 displays a schematic detailing the modifications. This work consisted of extension of the vacuum chamber (containing the QLT and the c-trap) such that it extended through the back panel of the instrument and housed an added 694.5 mm long octopole to which an NCI source was affixed. An existing RF supply module was modified to match the increased capacitance of the long octopole by placing a capacitor in the LC oscillator circuit. The vacuum chamber between the NCI source and the c-trap was pumped by an additional 70 L/s turbo pump (Pfeiffer Vacuum, Nashua, NH). Because the c-trap is by design held at ground during anion injection, the NCI source was electrically isolated and pulled slightly negative to create a continuous potential well between the NCI source and the QLT.

Initial experiments with the system were focused on anion transport and the development of a reagent anion injection scheme. To do this we measured the intensity of the fluoranthene radical anion as a function of voltage setting during anion injection for all the devices between the NCI source and the QLT (e.g., the DC potentials of the lenses and RF devices, Figure 3). After which the optimal values employed and code was written to automate the whole process (typical values shown in Figure 1). After optimization we note that the time necessary to accumulate an appropriate reagent anion density was four times that typically observed on a standalone QLT system – 1–2 ms vs. 4–8 ms. We attribute this difference mainly to the requirement that we pass anions through the c-trap. The c-trap was designed to accumulate, confine, and condition analyte ions, prior to injection into the orbitrap analyzer. Optimal operation therefore requires that the c-trap be held at relatively high pressure (up to 10^{-3} mbar of N_2) to guarantee efficient analyte ion trapping for downstream orbitrap *m/z* analysis. Operation at such pressures, however, is detrimental for anion reagent transport. To assess the affect of c-trap pressure on anion transmission and cation capture, the flow of N_2 into the c-trap was varied. The pressure was indirectly measured at an ion gauge located on the instrument vacuum manifold near the c-trap. Panel C of Figure 2 displays the expected result – the lower the pressure of N_2 the more intense the flux of anions. As the pressure measured in QLT chamber increased from 1.2×10^{-5} to 1.9×10^{-5} Torr, the intensity of anions fell approximately 40%. At the same time the efficiency of cation capture in the c-trap, as assessed by measuring the final intensity of cations to reach the orbitrap, increased almost 230%. Ultimately, a somewhat arbitrary compromise of 1.65×10^{-5} Torr was chosen. We note elevation of the pressure to 1.9×10^{-5} Torr produced a modest 8% increase in cation capture efficiency, but cost the anion transmission efficiency a further 25%.

Selection of the appropriate c-trap RF voltage presents a similar conundrum. By design the c-trap may only have a single RF voltage during an entire scan. Thus, even though the anion and cation injection periods are temporally separated, a compromise between analyte cation and anion transmission efficiency must be made. Ultimately, the capture of analyte cations was deemed more important as anion injection times can be extended. Panel D of Figure 2 shows

the effect of c-trap RF amplitude on anion injection efficiency. Typical operation requires the RF amplitude to be set at ~ 1500 V; however, if the c-trap RF amplitude were optimized for anion transmission, the efficiency would go up approximately 260%. Our inability to employ the optimal c-trap RF amplitude during anion injection and the requirement that the c-trap pressure remain high roughly account for the four fold difference in anion injection time between the standalone QLT system and this QLT-orbitrap system.

Complex mixture results

For large-scale protein sequencing applications, tandem MS duty cycle is a key figure of merit. In our FE-ETD implementation long anion injection times and poor ETD efficiencies necessitated spectral averaging and extremely long MS/MS duty cycles −6 seconds.[20] In that work we demonstrated compatibility with chromatography by analyzing a complex peptide mixtures via LC-MS/MS. A 45 minute gradient was used to separate the peptides and a data-dependent algorithm selected precursor ion *m/z* values for ETD fragmentation followed by with product ion *m/z* analysis in the orbitrap. From that analysis we identified only 34 unique peptides. To measure the effect of duty cycle and the efficiency of the new injection scheme we re-analyzed the same sample using identical chromatographic conditions. This time the resulting MS/MS spectra netted the identification of 269 unique peptides (false positive rate of 1%, Supplementary Table 1) – and 8 fold increase over the number of peptides identified by the FE-ETD injection scheme. This difference scales closely with the difference in duty cycle; one ETD analysis (i.e., two microscans) using the FE-ETD injection scheme required six seconds, whereas one ETD analysis (i.e., one microscan) with the NCI injection scheme required 0.8 seconds – a 7.5 fold decrease in duty cycle. Figure 3 displays four representative MS/MS spectra from this experiment. Panel A of Figure 3 displays the base peak chromatogram for all eluting peptides while Panel B displays the selected ion chromatograms for the four tandem mass spectra presented in Panels C through F. These single-scan FT ETD-MS/MS spectra have high S:N ratios and show complete or near-complete backbone fragmentation.

Low or high resolution ETD MS/MS spectra

Implementation of ETD on a QLT-orbitrap instrument allows for mass analysis of *c*- and $z^{\bullet}$-type product ions in either the QLT or orbitrap mass analyzer. Figure 4 displays representative peptide tandem mass spectra from a human whole cell lysate that were obtained following successive single-scans by ETD where mass analysis was performed in either the orbitrap (30,000 resolving power) or the QLT. In each case 8 of 10 backbone bonds were broken. We note that, regardless of mass analyzer choice, the relative abundance of the *c*- and $z^{\bullet}$-type fragment ions are nearly identical; however, as expected, the use of the orbitrap allows for acquisition of a high resolution and mass accuracy product ion spectra. For example, at a nominal resolving power of 30,000 the $z^{\bullet}_{9}$ ion is measured to within 1.3 ppm of its accurate mass in the orbitrap – this same ion is observed with 225 ppm mass error in the ion trap-acquired spectrum.

The heightened mass accuracy and resolution comes at the cost of scan speed and sensitivity. The average duration of individual tandem mass spectra collected in the orbitrap (30,000 resolving power) and the ion trap were 890 ms and 480 ms, respectively. For complex mixture analysis, however, MS/MS duty cycle (scans per second) is decisive as the number of identifications generally scales with the number of MS/MS spectra acquired. That said, the gains in identification rate for ETD spectra acquired at high mass accuracies have just begun to be evaluated.[30] Recently we have described that valence parity renders $z^{\bullet}$-type ions chemically distinct from *b*-, *c*-, and *y*-type ions.[31] And for ETD spectra acquired with mass accuracies better than 5 ppm, ion type and chemical compositions can frequently be determined from mass alone. Thus, the instrument described here, in combination with these capabilities, will present many new opportunities for automated sequence derivation, including *de novo*.

Isotope-encoded quantification

A major force driving the development of ETD was the need for an activation method compatible with labile PTMs. Protein phosphorylation, for example, is critical in cellular signaling and labile during collisional activation.[14, 32–34] For this reason technologies that can (1) globally characterize and (2) quantify protein phosphorylation sites are of critical importance. So far the various commercial implementations of ETD have enabled global protein characterization; the low resolving power offered by ion traps, however, renders the coupling of ETD with isotope-encoded quantification methods extremely difficult. Note this has nothing to do with ETD *per se*, rather ETD has primarily been implemented on ion trap mass spectrometers where resolution of the isotope clusters of multiply charged peptide ion pairs is often not possible.

Here we demonstrate the utility of the ETD-enabled QLT-orbitrap mass spectrometer to both sequence and quantify isotopically labeled phosphopeptides. Stable isotope labeling with amino acids in cell culture (SILAC) was used to incorporate a ^{13}/C labeled version of arginine into each protein of a control human cell population.[35–37] Proteins harvested from these cells were then mixed with a treatment group cultured under normal conditions. Following tryptic digestion and phosphopeptide enrichment, the sample was separated and sampled by the ETD-enabled QLT-orbitrap mass spectrometer where eluting peptides had their masses recorded using the orbitrap. Precursors were then selected in a data-dependent fashion and fragmented via ETD with subsequent QLT mass analysis. Panel A of Figure 5 displays the orbitrap full scan mass spectrum for an eluting phosphopeptide pair – the ions of 561.9394 and 563.9456 *m/z*. The chromatographic elution profiles of both *m/z* peaks is shown in Panel B of Figure 5. From these data we conclude the phosphopeptide is upregulated ~ five-fold upon treatment. Next the sequence of the upregulated peptide is determined from the ETD-MS/MS mass spectrum to be TGGKEAASGTtPQKSR (Figure 5, Panel C). This ETD spectrum was acquired in 400 ms and resulted in the production of 25 of 30 possible fragment ions. More importantly this sequence contains five sites that could harbor the phosphate group – cleavage of nearly every inter-residue bond allows for confident identification of the exact site.

Large peptide PTM analysis

In certain cases, PTMs decorate long stretches of proteins and the resulting patterns they create have biological relevance. There is no better example of such a case than histones – highly basic proteins that function to package DNA.[38, 39] The PTM patterns on the N-termini of these molecules are proposed to control gene regulation, i.e., the histone code hypothesis. It is, thus, critical to map these PTM patterns together and in the context of one another. In such applications ETD can be highly informative as it is more or less indifferent to peptide length or the presence of PTMs.[12, 25, 40, 41] Large peptides, however, are often multiply protonated, as are the resulting fragment ions. These spectra can be challenging to interpret when product ion *m/z* analysis is performed with an ion trap. To combat this, we and others have used a second ion/ion reaction to remove charge and simply the spectra (proton transfer).[12, 42–44] That strategy can be successful but will impose a mass limitation as the QLT typically measures mass up to 2000 *m/z*. The result is that only the N- and C-termini of the large peptide is measured.

We surmised that the mass resolving power offered by the orbitrap would negate the requirement of proton transfer for ETD product ion simplification. To test this hypothesis we gradient eluted a complex mixture of the highly modified N-terminal peptides from human histone H4 (residues 1–23, purified from human embryonic stem cells). Panel A of Figure 6 displays the LC-MS chromatogram of the N-terminal tail mixture. The major peaks are all unphosphorylated; however, a low level isoform eluting at about 18 minutes exhibited a precursor *m/z* that was consistent with the addition of 2 acetylations, 2 methylations, and one

phosphorylation (Panel B, Figure 6). This precursor was subsequently isolated and subjected to ETD followed product ion mass analysis in the orbitrap mass analyzer. Panel C of Figure 6 shows the single scan orbitrap *m/z* analysis of ETD fragments. All detected fragments lie between ~ 160 and 1300 *m/z*. From the well-resolved isotopic clusters, the spectrum is easily deconvoluted to produce the mass spectrum shown in Panel D of Figure 6. Here we see a simple spectrum of consecutive *c*- and $z^{\bullet}$-type products that allows one to read the sequence all the way to the total mass of 2,555 Da. Nearly every possible fragment ion is observed (39 out of 44 possible) in a scan that lasted for 1.14 seconds.

Intact protein identification

We reasoned that the ETD-enabled orbitrap mass spectrometer should likewise afford the opportunity to sequence intact proteins. First we performed a 15 ms ETD reaction of ubiquitin cations (+13) with fluoranthene anions in the QLT. The product ions produced from this reaction were subsequently deposited into the orbitrap (60,000 nominal resolving power) for *m/z* analysis. The resulting single-scan spectrum Figure 7, collected in 750 ms, contained 112 of 150 possible backbone fragments to yield 88% sequence coverage. Application of the ETD/PTR method for this same protein was previously described by some of us (JJC and JEPS).[12] In that experiment four single-scan spectra were averaged (~ 2 s) to yield only 28 of 150 possible fragments. From these data we conclude that our new system offers a viable alternative to PTR and is capable of sequencing proteins and peptides up to ~ 10 kDa on time-scales as short at 750 ms.

Figure 7 also displays the FT ETD-MS/MS analysis of a larger protein – myoglobin (Panel B). Here we subjected the +20 charge state of the 17 kDa protein to ETD followed by orbitrap *m/z* analysis. Spectra resulting from one, ten, and fifty scans were collected. Rich fragmentation spectra are generated in all cases, but unlike with ubiquitin, the single scan spectrum does not have sufficient S/N to permit *c*- and $z^{\bullet}$-type product ion identification. Only after ten scans are averaged (data not shown) do the isotopic clusters begin to appear. Inspection of fifty averaged scans (Figure 7, panel B) revealed 127 of 304 possible backbone fragments, translating to 55% sequence coverage. As evident from these data, as protein mass increases there is a concomitant increase both the number of dissociation channels (i.e., number of possible *c*- and $z^{\bullet}$-type products) and isotopic complexity. The result is an apparent lowering of S/N that must be compensated by spectral averaging.

Conclusions

Here we describe the modification of an orbitrap mass spectrometer to accommodate a NCI source for reagent anion generation. We demonstrate the device to allow for the rapid and robust injection of fluoranthene radical anions (~ 4 – 8 ms) into the QLT for conducting ETD ion/ion reactions. Once deposited ETD reactions are conducted in the QLT, followed by product ion *m/z* analysis in either the QLT or orbitrap. We tested the applicability of this new system to a variety of contemporary proteomic problems including – complex mixture analysis, PTM site localization, stable isotope-based quantitation, large peptide analysis, and top-down proteomics. Use of the orbitrap analyzer for product ion *m/z* analysis provides sufficient sensitivity to permit single-scan analysis, but comes mainly at the price of speed (as compared to QLT *m/z* analysis). Even when the QLT is employed for ETD product ion *m/z* analysis, the mass resolution and accuracy afforded by the orbitrap full MS spectrum is highly useful for confirming putative sequence candidates and for quantifying isotopically labeled peptide pairs. Large peptide and whole protein characterization technologies are still developing and represent a point of growth in the proteomics field. From the data presented herein we conclude the ETD-enabled orbitrap will become an important tool in this regard.

The coupling of ETD with the high mass accuracy orbitrap mass analyzer will also offer several new opportunities. For example, the current instrument configuration is easily adapted to blend both collisional (CAD) and chemical (ETD) dissociation methods in a data-dependent fashion.[45] Such operation can significantly boost the probability of a successful sequencing outcome by tailoring the dissociation method to each precursor *m/z*. A second prospect lies in the collection of accurate mass ETD spectra. We recently reported that valence parity renders $z^{\bullet}$-type ions chemically distinct from *b*-, *c*-, and *y*-type ions.[31] This means that with mass measurement accuracies of a few ppm, one can directly annotate ETD tandem mass spectra with ion type information. Here we show that the ETD-enabled orbitrap system can acquire such spectra in less than one second each, in an unsupervised, data-dependent fashion. With the appropriate software, we predict these spectra will provide an excellent foundation from which to directly determine sequence (*de novo*).[46–48]

Acknowledgements

We thank Paul Bertics, Sam Hozer, and April Jue for culture and harvest of the human glioblastoma cell line and Kai Meier for mechanical design of vacuum chamber and octopole. The University of Wisconsin-Madison, Thermo Scientific, the Beckman Foundation, the American Society of Mass Spectrometry, Eli Lilly, the National Science Foundation (0701846; 0747990 both to JJC), and the NIH (1R01GM080148 to JJC) provided financial support for this work. GCM, DP, and DLS gratefully acknowledge support from NIH pre-doctoral fellowships – (Biotechnology Training Program, NIH 5T32GM08349, to GCM; the Genomic Sciences Training Program, NIH 5T32HG002706, to DP and DLS).

References

1. Syka JEP, Marto JA, Bai DL, Horning S, Senko MW, Schwartz JC, Ueberheide B, Garcia B, Busby S, Muratore T, Shabanowitz J, Hunt DF. Journal of Proteome Research 2004;3:621–626. [PubMed: 15253445]
2. Makarov A, Denisov E, Lange O, Horning S. Journal of the American Society for Mass Spectrometry 2006;17:977–982. [PubMed: 16750636]
3. Makarov A, Denisov E, Kholomeev A, Baischun W, Lange O, Strupat K, Horning S. Analytical Chemistry 2006;78:2113–2120. [PubMed: 16579588]
4. Yates JR, Cociorva D, Liao LJ, Zabrouskov V. Analytical Chemistry 2006;78:493–500. [PubMed: 16408932]
5. Ong SE, Mann M. Nature Chemical Biology 2005;1:252–262.
6. Hunt DF, Yates JR, Shabanowitz J, Winston S, Hauer CR. Proceedings of the National Academy of Sciences of the United States of America 1986;83:6233–6237. [PubMed: 3462691]
7. Coon JJ, Syka JE, Shabanowitz J, Hunt DF. Biotechniques 2005;38:519, 521, 523. [PubMed: 15884666]
8. Swaney DL, McAlister GC, Wirtala M, Schwartz JC, Syka JEP, Coon JJ. Analytical Chemistry 2007;79:477–485. [PubMed: 17222010]
9. Good DM, Wirtala M, McAlister GC, Coon JJ. Mol Cell Proteomics. 2007
10. Good DM, Coon JJ. Biotechniques 2006;40:783–789. [PubMed: 16774122]
11. Coon JJ, Shabanowitz J, Hunt DF, Syka JEP. Journal of the American Society for Mass Spectrometry 2005;16:880–882. [PubMed: 15907703]
12. Coon JJ, Ueberheide B, Syka JEP, Dryhurst DD, Ausio J, Shabanowitz J, Hunt DF. Proceedings of the National Academy of Sciences of the United States of America 2005;102:9463–9468. [PubMed: 15983376]
13. Coon JJ, Syka JEP, Schwartz JC, Shabanowitz J, Hunt DF. International Journal of Mass Spectrometry 2004;236:33–42.
14. Syka JEP, Coon JJ, Schroeder MJ, Shabanowitz J, Hunt DF. Proceedings of the National Academy of Sciences of the United States of America 2004;101:9528–9533. [PubMed: 15210983]
15. Chrisman PA, Pitteri SJ, Hogan JM, McLuckey SA. Journal of the American Society for Mass Spectrometry 2005;16:1020–1030. [PubMed: 15914021]

16. Pitteri SJ, Chrisman PA, Hogan JM, McLuckey SA. Analytical Chemistry 2005;77:1831–1839. [PubMed: 15762593]
17. Pitteri SJ, Chrisman PA, McLuckey SA. Analytical Chemistry 2005;77:5662–5669. [PubMed: 16131079]
18. Field FH. Accounts of Chemical Research 1968;1:42.
19. Hunt DF, Crow FW. Analytical Chemistry 1978;50:1781–1784.
20. McAlister GC, Phanstiel D, Good DM, Berggren WT, Coon JJ. Analytical Chemistry 2007:3525–3534. [PubMed: 17441688]
21. Liang XR, Xia Y, McLuckey SA. Analytical Chemistry 2006;78:3208–3212. [PubMed: 16643016]
22. Xia Y, Chrisman PA, Erickson DE, Liu J, Liang XR, Londry FA, Yang MJ, McLuckey SA. Analytical Chemistry 2006;78:4146–4154. [PubMed: 16771545]
23. Williams DK Jr, McAlister GC, Good DM, Coon JJ, Muddiman DC. Anal Chem 2007;79:7916–7919. [PubMed: 17867655]
24. Martin SE, Shabanowitz J, Hunt DF, Marto JA. Analytical Chemistry 2000;72:4266–4274. [PubMed: 11008759]
25. Phanstiel D, Brumbaugh J, Berggren WT, Conard KR, Feng X, Levenstein ME, McAlister GC, Thomson JA, Coon JJ. Proc Natl Acad Sci U S A 2008;105:4093–4098. [PubMed: 18326628]
26. Ludwig TE, Bergendahl V, Levenstein ME, Yu JY, Probasco MD, Thomson JA. Nature Methods 2006;3:637–646. [PubMed: 16862139]
27. Villen J, Beausoleil SA, Gerber SA, Gygi SP. Proceedings of the National Academy of Sciences of the United States of America 2007;104:1488–1493. [PubMed: 17242355]
28. Geer LY, Markey SP, Kowalak JA, Wagner L, Xu M, Maynard DM, Yang XY, Shi WY, Bryant SH. Journal of Proteome Research 2004;3:958–964. [PubMed: 15473683]
29. Elias JE, Gygi SP. Nature Methods 2007;4:207–214. [PubMed: 17327847]
30. Liu J, Liang XR, McLuckey SA. Journal of Proteome Research 2008;7:130–137. [PubMed: 17997514]
31. Hubler SL, Jue A, Keith J, McAlister GC, Craciun G, Coon JJ. J Am Chem Soc. 2008
32. Chi A, Huttenhower C, Geer LY, Coon JJ, Syka JEP, Bai DL, Shabanowitz J, Burke DJ, Troyanskaya OG, Hunt DF. Proceedings of the National Academy of Sciences of the United States of America 2007;104:2193–2198. [PubMed: 17287358]
33. Molina H, Horn DM, Tang N, Mathivanan S, Pandey A. Proceedings of the National Academy of Sciences of the United States of America 2007;104:2199–2204. [PubMed: 17287340]
34. Mann M, Jensen ON. Nature Biotechnology 2003;21:255–261.
35. Gruhler A, Olsen JV, Mohammed S, Mortensen P, Faergeman NJ, Mann M, Jensen ON. Molecular & Cellular Proteomics 2005;4:310–327. [PubMed: 15665377]
36. Ong SE, Kratchmarova I, Mann M. Journal of Proteome Research 2003;2:173–181. [PubMed: 12716131]
37. Ong SE, Blagoev B, Kratchmarova I, Kristensen DB, Steen H, Pandey A, Mann M. Molecular & Cellular Proteomics 2002;1:376–386. [PubMed: 12118079]
38. Fischle W, Wang YM, Allis CD. Current Opinion in Cell Biology 2003;15:172–183. [PubMed: 12648673]
39. Strahl BD, Allis CD. Nature 2000;403:41–45. [PubMed: 10638745]
40. Ueberheide BM, Mollah S. International Journal of Mass Spectrometry 2007;259:46–56.
41. Taverna SD, Ueberheide BM, Liu YF, Tackett AJ, Diaz RL, Shabanowitz J, Chait BT, Hunt DF, Allis CD. Proceedings of the National Academy of Sciences of the United States of America 2007;104:2086–2091. [PubMed: 17284592]
42. Stephenson JL, McLuckey SA. Analytical Chemistry 1998;70:3533–3544. [PubMed: 9737205]
43. McLuckey SA, Stephenson JL. Mass Spectrometry Reviews 1998;17:369–407. [PubMed: 10360331]
44. Chi A, Bai DL, Geer LY, Shabanowitz J, Hunt DF. International Journal of Mass Spectrometry 2007;259:197–203. [PubMed: 17364019]
45. McAlister, GC.; Makarov, A.; Horning, S.; Phanstiel, D.; Swaney, DL.; Syka, JE.; Stafford, GC.; Lange, O.; Coon, JJ. Indianapolis, IN: 2007.

46. Frank AM, Savitski MM, Nielsen ML, Zubarev RA, Pevzner PA. Journal of Proteome Research 2007;6:114–123. [PubMed: 17203955]

47. Spengler B. European Journal of Mass Spectrometry 2007;13:83–87. [PubMed: 17878544]

48. Savitski MM, Nielsen ML, Kjeldsen F, Zubarev RA. Journal of Proteome Research 2005;4:2348–2354. [PubMed: 16335984]

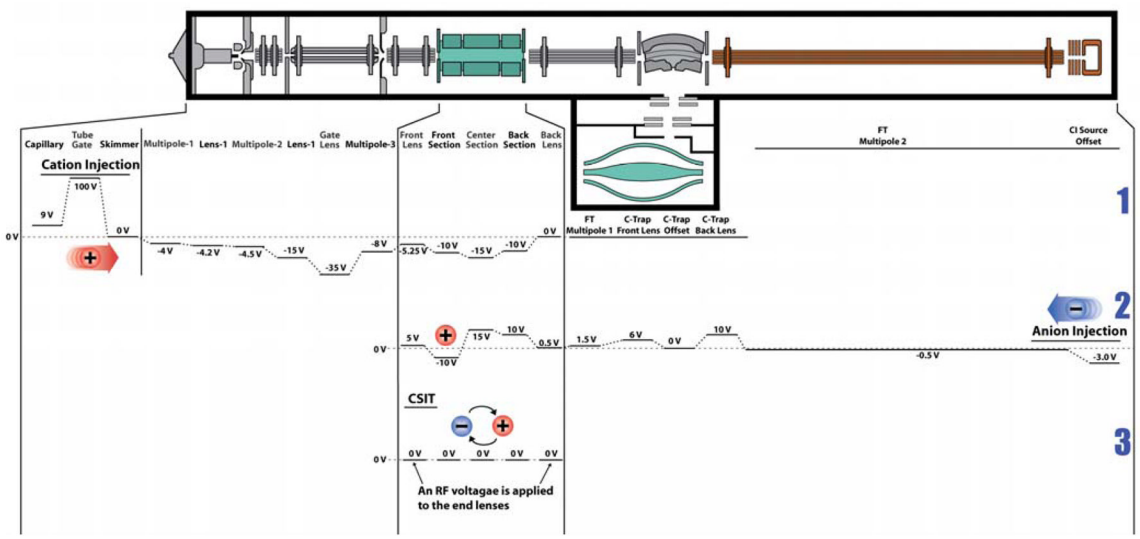

Figure 1.

Schematic of the ETD-enabled QLT-orbitrap hybrid mass spectrometer. The mass analyzers are highlighted in green, while the added components, for ETD, are highlighted in orange. The lift-out information below the figure details the voltages used during (1) cation injection, (2) anion injection, and (3) ion/ion reaction.

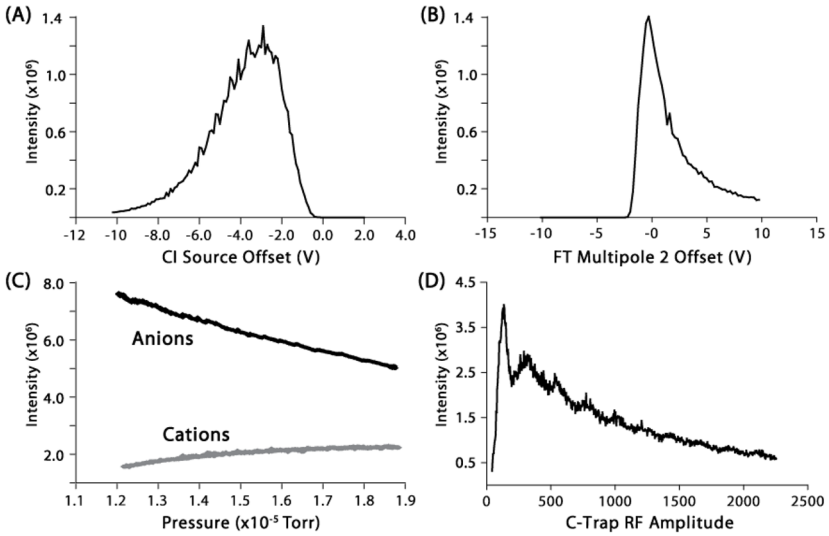

Figure 2.

Panels A and B display plots of anion reagent intensity as a function of either CI source offset or FT Multipole 2 offset, respectively. Panel C displays the measured signal of both an anion and cation population as a function of c-trap pressure. Note we wish to operate the device to maximize both. The pressure inside the c-trap was adjusted by varying the flow on N_2 into the device and was indirectly measured using an ion gauge located outside of the device, on the vacuum manifold wall of the instrument. Anion intensity was measured using the QLT and cation intensity was measured with the orbitrap. Panel B plots the anion reagent intensity as a function of c-trap RF amplitude.

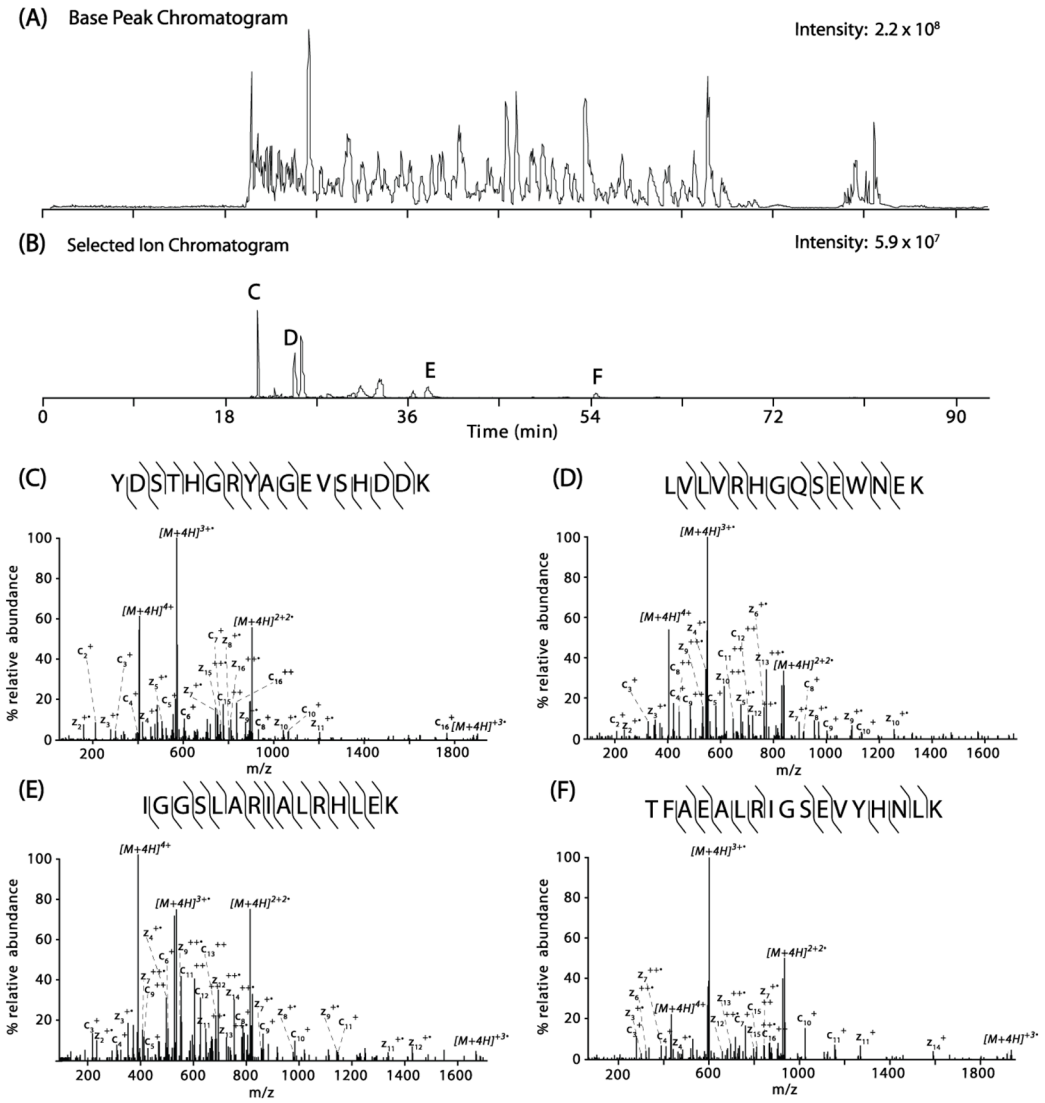

Figure 3.

nHPLC-MS analysis of a Lys-C digested yeast protein sample. An automated data-dependent analysis was designed to first sample the eluent by full-MS using the orbitrap mass analyzer followed by ETD MS/MS with orbitrap analysis.

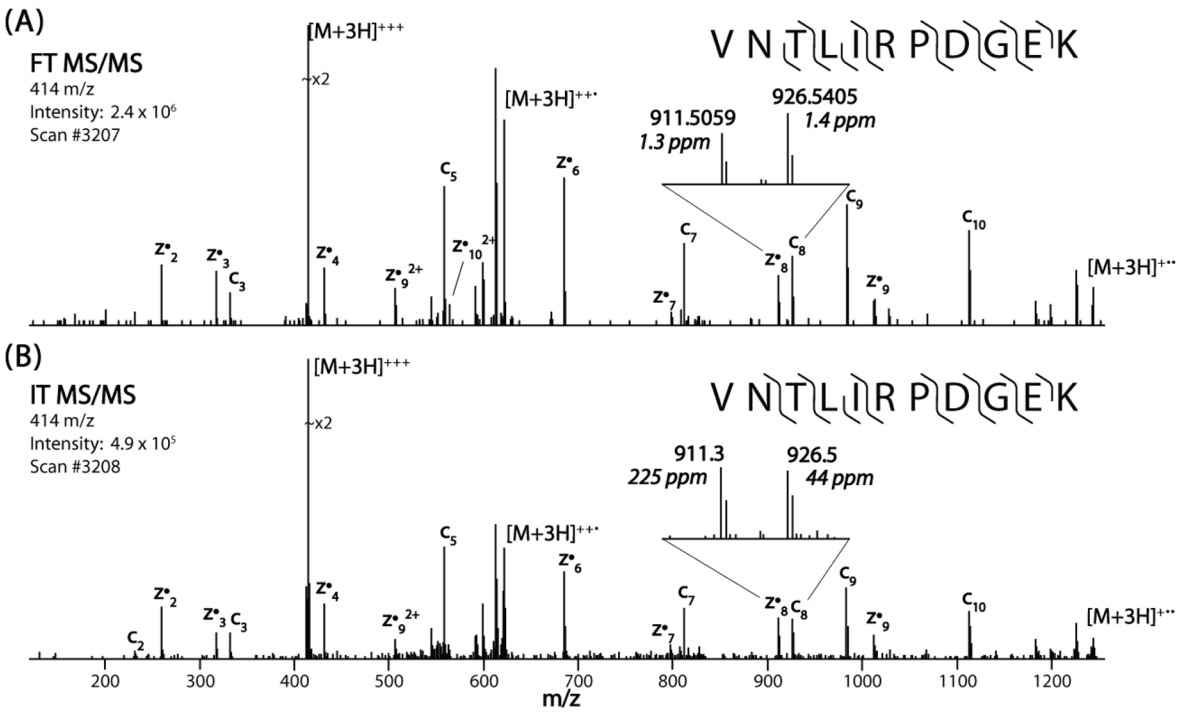

Figure 4.

A triply protonated peptide having the sequence VNTLIRPDGEK was subjected to ETD fragmentation and *m/z* analyzed using either the (A) orbitrap or (B) the ion trap mass analyzer. Aside from the increased mass resolution and accuracy achieved when using the oribtrap, the single-scan spectra are nearly identical.

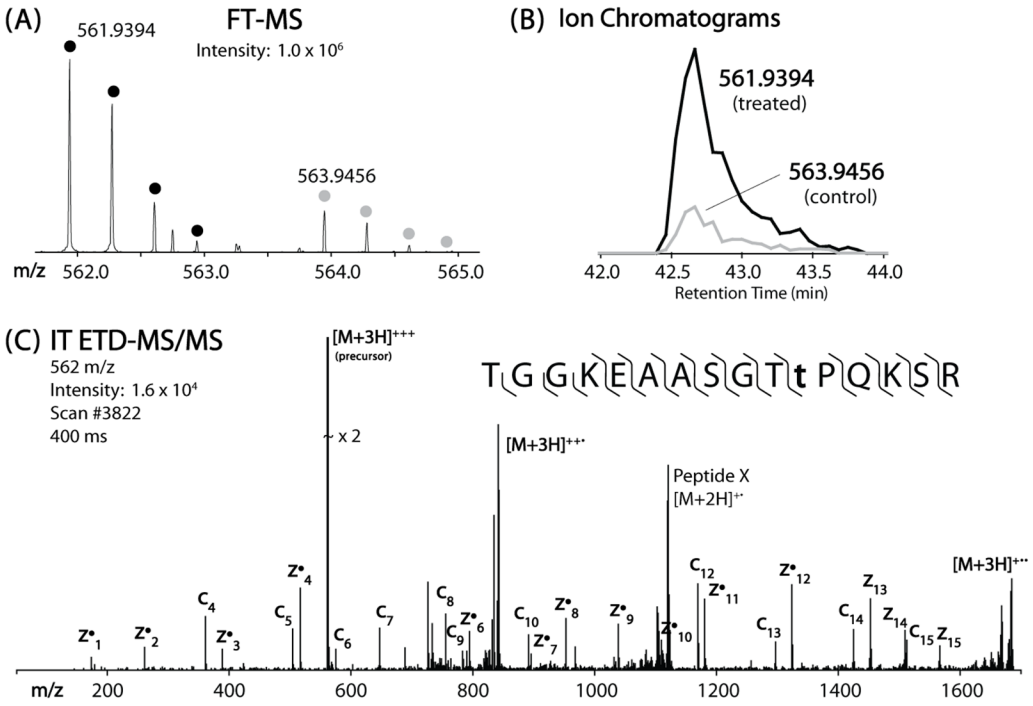

Figure 5.

The full-MS spectrum of a SILAC-labeled peptide pair is shown in Panel A. The orbitrap affords excellent mass resolution and accuracy so that the pair is easily distinguished from one another. Panel B displays the selected ion chromatograms for these two species. The ETD-MS/MS spectrum was acquired using the ion trap and is presented in Panel C. From this spectrum we can easily deduce sequence and localize the site of phosphorylation (**t**); and, from the selected ion chromatogram (Panel B), we conclude this phosphorylation site is upregulated ~ 5-fold.

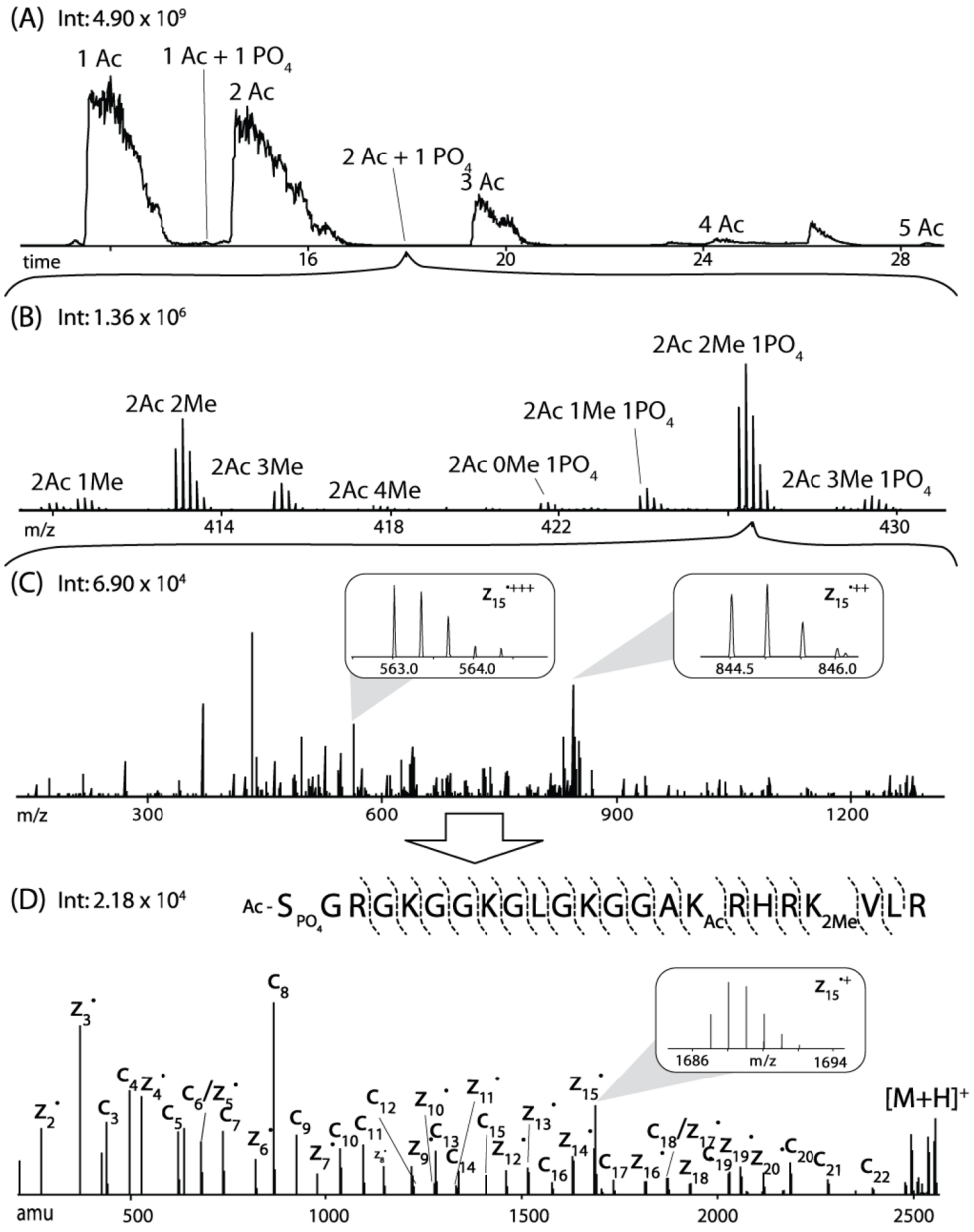

Figure 6.

Panel A displays the nHPLC chromatogram of Asp-N digested human histone H4. A full-MS spectrum of peaks eluting at approximately 18 minutes is shown in Panel B. Eight clusters of *m/z* peaks are observed representing eight differently modified isoforms of the N-terminal tail of histone H4. The peak of 426 *m/z* was isolated and subjected to a 50 ms ETD reaction in the QLT (Panel C). Fragment ions were detected using the orbitrap mass analyzer. The ETD reaction resulted in the formation of numerous multiply charged m/z peaks that were resolved using the orbitrap and then converted to singly charged peaks using an deconvolution algorithm (Panel D). This spectrum is highly simplified and displays the near-complete sequence coverage of the peptide and unambiguous assignment of PTM locations.

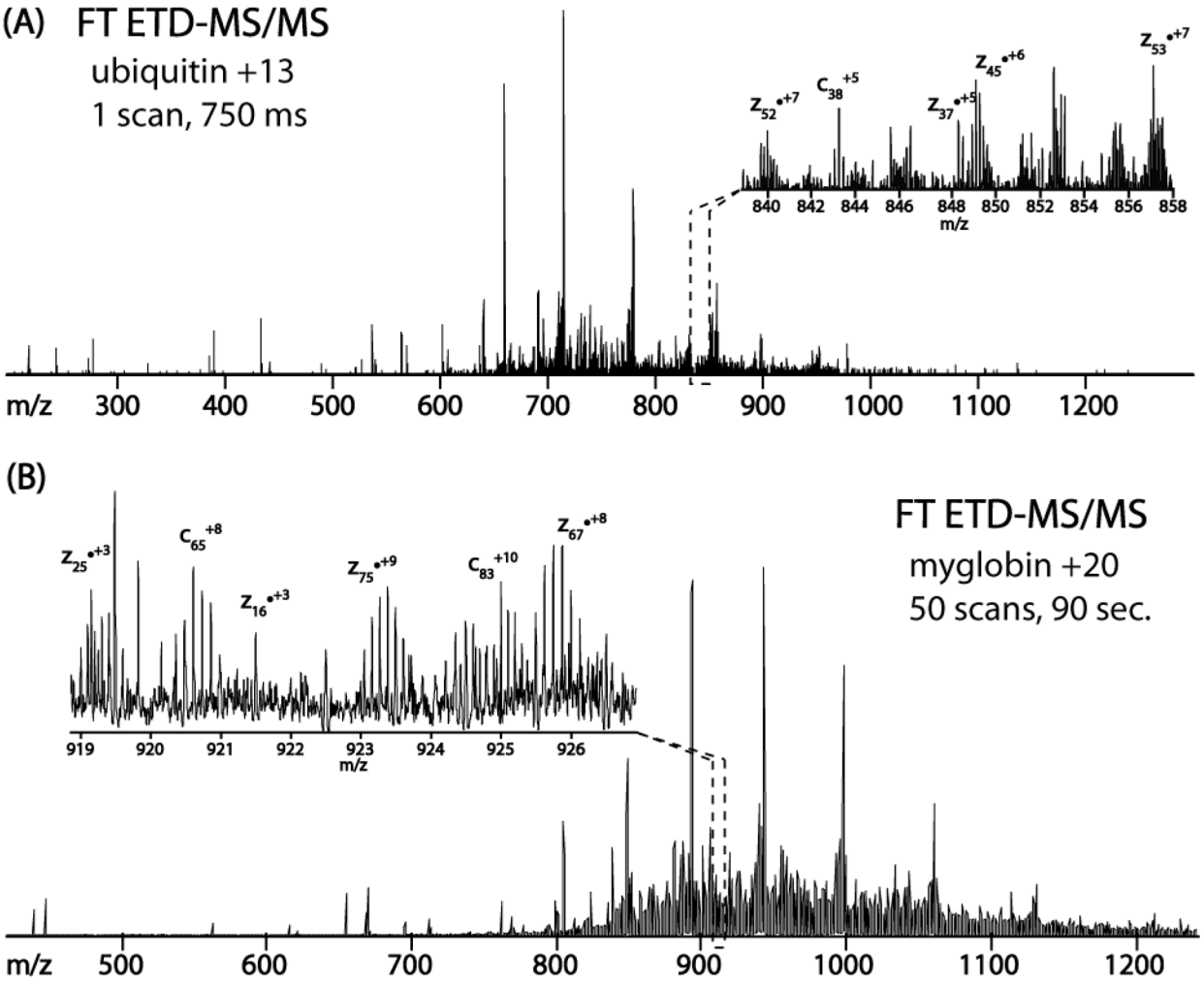

Figure 7.

Panel A presents a FT ETD-MS/MS single scan spectrum of the ubiquitin +13 precursor (m/z 659). This spectrum was collected in 750 ms and harbored 112 of 150 possible backbone fragments to yield 88% sequence coverage. The +20 charge state of myoglobin, a 17 kDa protein, was subjected to ETD followed by orbitrap *m/z* analysis. Inspection of the spectra, fifty averaged scans, revealed 127 of 304 possible backbone fragments, translating to 55% sequence coverage.